

2016

Proportional-Integral Extremum Seeking for Optimizing Power of Vapor Compression Systems

Daniel J Burns

Mitsubishi Electric Research Laboratories, United States of America, burns@merl.com

Christopher R. Laughman

Mitsubishi Electric Research Laboratories, United States of America, laughman@merl.com

Martin Guay

Queen's University, Ontario, Canada, martin.guay@chee.queensu.ca

Follow this and additional works at: <http://docs.lib.purdue.edu/iracc>

Burns, Daniel J; Laughman, Christopher R.; and Guay, Martin, "Proportional-Integral Extremum Seeking for Optimizing Power of Vapor Compression Systems" (2016). *International Refrigeration and Air Conditioning Conference*. Paper 1751.
<http://docs.lib.purdue.edu/iracc/1751>

This document has been made available through Purdue e-Pubs, a service of the Purdue University Libraries. Please contact epubs@purdue.edu for additional information.

Complete proceedings may be acquired in print and on CD-ROM directly from the Ray W. Herrick Laboratories at <https://engineering.purdue.edu/Herrick/Events/orderlit.html>

Proportional–Integral Extremum Seeking for Optimizing Power of Vapor Compression Systems

Daniel J. BURNS^{1*}Christopher R. LAUGHMAN¹Martin GUAY²

¹Mitsubishi Electric Research Laboratories
Cambridge, MA, USA

burns@merl.com, laughman@merl.com

*corresponding author

²Queen's University
Department of Chemical Engineering
Kingston, Ontario
martin.guay@chee.queensu.ca

ABSTRACT

While traditional perturbation-based extremum seeking controllers (ESC) for vapor compression systems have proven effective at optimizing power without requiring a process model, the algorithm's requirement for multiple distinct timescales has limited the applicability of this method to laboratory tests where boundary conditions can be carefully controlled, or simulation studies with unrealistic convergence times. In this paper, we optimize power consumption through the application of a newly-developed proportional–integral extremum seeking controller (PI-ESC) that converges *at the same timescale* as the process. This method uses an improved gradient estimation routine previously developed by the authors but also modifies the control law part of the algorithm to include terms proportional to the estimated gradient. PI-ESC is applied to the problem of compressor discharge temperature selection for a vapor compression system so that power consumption is minimized. We test the performance of this method using a custom-developed model of a vapor compression system written in the Modelica object-oriented modeling language. We compare the convergence times of PI-ESC to our previously developed time-varying ESC method and the conventional perturbation-based ESC method. For the conditions tested, PI-ESC is shown to converge to the optimum in about 15 minutes, whereas TV-ESC converges in 45 minutes and perturbation ESC requires more than 7,000 minutes due to its inefficient estimation of the gradient. Because of the improved convergence properties of PI-ESC, self-optimization algorithms for HVAC equipment can be deployed into situations where previous methods have failed.

1 INTRODUCTION

Vapor compression machines (Fig. 1A) move thermal energy from a low temperature zone to a high temperature zone, performing either cooling or heating depending on the configuration of the refrigerant piping. The relative simplicity of the machine and its effective and robust performance has enabled the vapor compression machine in various forms and packages to become widely deployed, and it is critical to modern comfort standards and the global food production and distribution industries. The wide-scale deployment of systems with variable control authority actuators (variable speed compressors, electronically positioned expansion valves, *etc.*) have created new opportunities for control methods to optimize performance. Additionally, market pressure has driven VCS manufacturers to reduce the number of actuators and sensors where possible (Gopal *et al.* (2014)). As a result of these trends, there are emerging opportunities for more advanced control of variable-actuation vapor compression systems, but these new strategies must conform to the restrictions imposed by a limited number of sensors available.

In many control formulations for vapor compression machines the evaporator superheat temperature is selected as a regulated variable for cycle efficiency and equipment protection (Elliott and Rasmussen (2010), Otten (2010), Vinther *et al.* (2013)). However, due to the economic pressures previously mentioned, direct measurement of superheat is not always available. Instead, this paper considers systems wherein the compressor discharge temperature is used as a surrogate for cycle efficiency. In many systems, the discharge temperature is often measured for equipment protection;

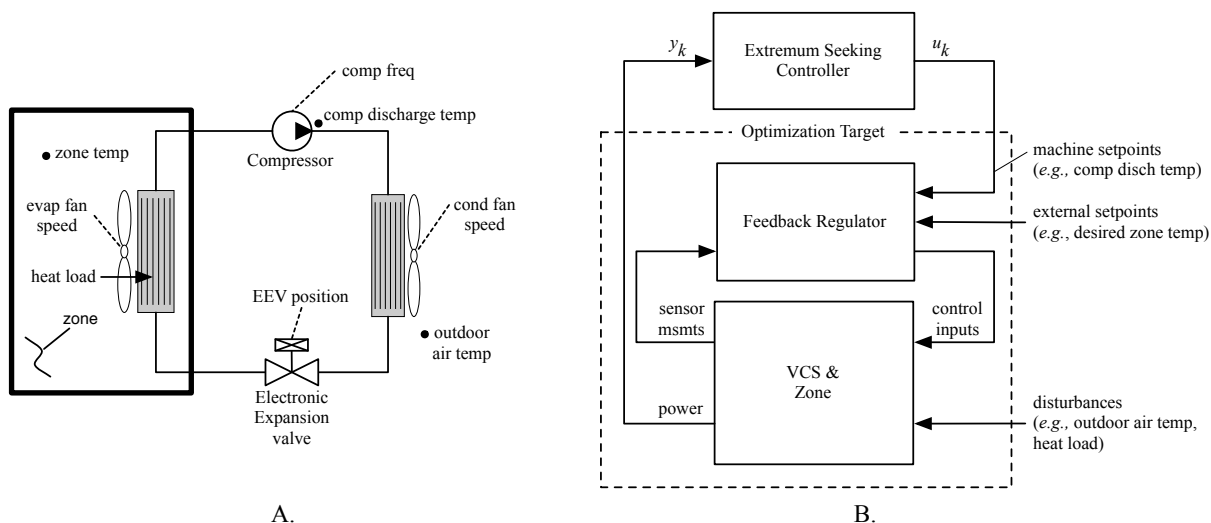


Figure 1: (A) Piping diagram of the multi-evaporator vapor compression system considered in this work. (B) Block diagram representing the signal-level interconnection between the vapor compression system and associated zone dynamics, the feedback regulator and the extremum seeking controller.

and because the refrigerant state at this location in the cycle is always superheated, this signal is a one-to-one function of the disturbances over the full range of expected operating points (Burns *et al.* (2015)). (Contrast this to evaporator superheat which is undefined for values less than zero, and therefore provides no sensible information for feedback controllers when the refrigerant state exiting the evaporator is two-phase.) Because the optimal discharge temperature changes with heat load and outdoor air temperature, its setpoint cannot be regulated to a constant, and instead must vary based on the external conditions. It is the aim of this paper to automate the generation of such setpoints in order to maximize energy efficiency using a class of model-free online optimization algorithms called extremum seeking.

Extremum seeking control (ESC) is a feedback control algorithm wherein the control objective is to obtain an input that minimizes or maximizes (“extremizes”) a performance metric without knowledge or a model of the process. Fig. 1B shows the realtime optimization problem addressed in this work. An extremum seeking controller is applied to an optimization target that consists of the vapor compression system and associated zone dynamics under the direction of a feedback regulator. The feedback regulator selects control inputs (compressor speed commands, expansion valve positions, *etc.*) that drive the system to setpoints that consist of (i) a desired zone temperature provided by an occupant, and (ii) machine setpoints such as a desired compressor discharge temperature. As previously described, the compressor discharge temperature influences the particular steady state operating point and therefore is the single variable in this controller architecture correlated to efficiency. Note that because the feedback regulator is multivariable and inputs to the vapor compression system couple to the outputs, modifying the (single) discharge temperature setpoint will cause the closed loop system to modify *all* control inputs. Therefore, selecting the optimal discharge temperature will determine the entire set of control inputs that minimize energy consumption.

However, determining this energy-optimal discharge temperature is not straightforward. Typical methods for maximizing the energy efficiency rely on the use of mathematical models of the physics of vapor compression systems. These model-based approaches attempt to describe the influence of commanded inputs on the thermodynamic behavior of the system and the resultant consumed energy, and they are used to predict the combination of inputs that both meets the heat load requirements and minimizes energy. However, these models of vapor compression systems rely on simplifying assumptions in order to produce a mathematically tractable representation. These assumptions often ignore important effects or do not consider installation-specific characteristics or time-varying effects, causing the model of the system to deviate from actual behavior of the installed system over time. Additionally, the variation in these systems during the manufacturing process are often so large as to produce vapor compression systems of the

same type that exhibit different input-output characteristics, and therefore a single model cannot accurately describe the variations among copies produced as the outcome of a stochastic manufacturing process. Finally, model-based optimization methods are difficult to derive and calibrate, and often do not describe variations over long time scales, such as those due to refrigerant losses or accumulation of debris on the heat exchangers.

Recently, model-free extremum seeking methods that operate in realtime and aim to optimize a cost have received increased attention and have demonstrated improvements in the optimization of vapor compression systems and other HVAC applications (Burns and Laughman (2012), Guay and Burns (2014), Li *et al.* (2010), Sane *et al.* (2006), Tyagi *et al.* (2006)). To date, the dominant extremum seeking algorithm that appears in the HVAC research literature is the traditional perturbation-based algorithm first developed in the 1920s (Leblanc (1922)) and re-popularized in the late 1990s by an elegant proof of convergence for a general class of nonlinear systems (Krstic (2000)).

Most extremum seeking controllers can be viewed as a gradient descent optimization algorithm implemented as a feedback controller and therefore consists of two main functional components: (i) a estimation part that determines the local gradient of the performance metric with respect to the decision variables, and (ii) a control law part that manipulates the decision variables to steer the system to the optimum of the performance metric. In the traditional perturbation-based method, a sinusoidal term is added to the input at a slower frequency than the natural plant dynamics, inducing a sinusoidal response in the performance metric (Tan *et al.* (2010)) and introducing a timescale slower than the process dynamics. The controller then filters and averages this signal to obtain an estimate of the gradient. Averaging the perturbation introduces yet another (and slower) time scale in the optimization process. Using a gradient estimate obtained in this way, the control law integrates the estimated gradient to drive the gradient to zero. As a result, the traditional perturbation-based extremum seeking converges to the neighborhood of the optimum at about two timescales slower than the plant dynamics due to inefficient estimation of the gradient, and slow (integral-action dominated) adaptation in the control law. For thermal systems such as vapor compression machines where the dynamics are already on the order of tens of minutes, the slow convergence properties of perturbation-based extremum seeking are impediments to wide-scale deployment.

However, convergence rates can be improved by addressing both components of the extremum seeking algorithm. A more efficient method for estimating gradients has been developed that treats the gradient as an unknown time-varying parameter to be identified. Time-varying extremum seeking (TV-ESC) uses adaptive filtering techniques to estimate the parameters of the gradient—eliminating the timescale associated with averaging perturbations (Guay (2014)). Recently, the authors successfully applied this technique to vapor compression system optimization (Weiss *et al.* (2014)). However, that method did not modify the control law, and while convergence was significantly improved compared to the perturbation-based method, the control law of TV-ESC is still integral-action dominated.

This paper presents the development of a new proportional-integral extremum seeking controller in which the control law includes terms proportional to the estimated gradient, and the estimation routine is modified to avoid bias introduced by this control law. This results in an online model-free optimization routine that converges at the same timescale as the dominant system time constant. The PI-ESC algorithm is presented in Section 2 and demonstrated in a comparison on a simple example in Section 3. A brief description of the custom-written model used to demonstrate effectiveness of the proposed approach is provided in Section 4, followed by simulation results in Section 5.

2 PROPORTIONAL-INTEGRAL EXTREMUM SEEKING

This section outlines the development of an extremum seeking controller based on a time-varying estimate of the gradient of the cost and a PI control law to drive the system to its optimum operating point. See Guay and Burns (2015) for the full development and stability and convergence analysis in discrete time.

We consider a class of nonlinear systems of the form:

$$x_{k+1} = x_k + f(x_k) + g(x_k)u_k \quad (1)$$

$$y_k = h(x_k) \quad (2)$$

where $x_k \in \mathbb{R}^n$ is the vector of state variables at time k , u_k is the input variable at time k taking values in $\mathcal{U} \subset \mathbb{R}$ and $y_k \in \mathbb{R}$ is the objective function at step k , to be minimized. It is assumed that $f(x_k)$ and $g(x_k)$ are smooth vector valued functions and that $h(x_k)$ is a smooth function.

We assume that the cost $h(x)$ is relative order one and satisfies the optimality conditions:

$$\frac{\partial h(x^*)}{\partial x} = 0 \quad (3)$$

$$\frac{\partial^2 h(x)}{\partial x \partial x^T} > \beta I, \quad \forall x \in \mathbb{R}^n \quad (4)$$

where β is a strictly positive constant.

We let $\alpha(x_k, \hat{u}_k) = x_k + f(x_k) + g(x_k)\hat{u}_k$. The rate of change of the cost function $y_k = h(x_{k+1})$ is given by:

$$h(x_{k+1}) - h(x_k) = h(x_k + f(x_k) + g(x_k)u_k) - h(\alpha(x_k)) + h(\alpha(x_k), \hat{u}_k) - h(x_k).$$

Using a second order Taylor expansion on the first two terms we can rewrite the cost dynamics as:

$$y_{k+1} - y_k = \Psi_{0,k}(x_k, \hat{u}_k) + \Psi_{1,k}(x_k, u_k, \hat{u}_k)(u_k - \hat{u}_k).$$

where $\Psi_{0,k}(x_k, \hat{u}_k) = h(\alpha(x_k, \hat{u}_k)) - h(x_k)$, and $\Psi_{1,k}(x_k, u_k, \hat{u}_k) = (\nabla h(\alpha(x_k, \hat{u}_k))g(x_k) + \frac{1}{2}(u_k - \hat{u}_k)^\top g(x_k)^\top \nabla^2 h(\tilde{y}_k)g(x_k)$ where $\tilde{y}_k = \alpha(x_k, \hat{u}_k) + \theta g(x_k)(u_k - \hat{u}_k)$ for $\theta \in (0, 1)$. By the relative order one assumption on $h(x)$, the system's dynamics can be decomposed and written as:

$$\xi_{k+1} = \xi_k + \psi(\xi_k, y_k) \quad (5)$$

$$y_{k+1} = y_k + \Psi_{0,k}(x_k, \hat{u}_k) + \Psi_{1,k}(x_k, u_k, \hat{u}_k)(u_k - \hat{u}_k) \quad (6)$$

where $\xi_k \in \mathbb{R}^{n-1}$ and $\psi(\xi_k, y_k)$ is a smooth vector valued function. By Equation (6), the cost function dynamics are parameterized as follows:

$$y_{k+1} = y_k + \theta_{0,k} + \theta_{1,k}(u_k - \hat{u}_k)$$

where the time-varying parameters $\theta_{0,k}$ and $\theta_{1,k}$ represent $\Psi_{0,k}$ and $\Psi_{1,k}$, and are to be identified. Importantly, in order to estimate the gradient $\theta_{1,k}$ without bias, $\theta_{0,k}$ must also be determined.

Let $\hat{\theta}_{0,k}$ and $\hat{\theta}_{1,k}$ denote the estimates of $\theta_{0,k}$ and $\theta_{1,k}$, respectively, and consider the following state predictor

$$\hat{y}_{k+1} = \hat{y}_k + \hat{\theta}_{0,k} + \hat{\theta}_{1,k}(u_k - \hat{u}_k) + K_k e_k - \omega_{k+1}(\hat{\theta}_k - \hat{\theta}_{k+1}) \quad (7)$$

where $\hat{\theta}_k = [\hat{\theta}_{0,k}, \hat{\theta}_{1,k}^\top]^\top$ is the vector of parameter estimates at time step k given by any update law, K_k is a correction factor at time step k , $e_k = y_k - \hat{y}_k$ is the state estimation error. We let $\phi_k = [1, (u_k - \hat{u}_k)^\top]^\top$. The variable w_k is the following output filter at time step k

$$w_{k+1} = w_k + \phi_k - K_k w_k, \quad (8)$$

with $\omega_0 = 0$. Using the state predictor defined in (7) and the output filter defined in (8), the prediction error $e_k = y_k - \hat{y}_k$ is given by

$$\begin{aligned} e_{k+1} &= e_k + \phi_k \tilde{\theta}_{k+1} - K_k e_k + \omega_{k+1}(\hat{\theta}_k - \hat{\theta}_{k+1}) + w_{k+1}(\theta_{k+1} - \theta_k) \\ e_0 &= y_0 - \hat{y}_0. \end{aligned} \quad (9)$$

An auxiliary variable η_k is introduced which is defined as $\eta_k = e_k - w_k^\top \tilde{\theta}_k$. Its dynamics are given by

$$\begin{aligned} \eta_{k+1} &= e_{k+1} - w_{k+1}^\top \tilde{\theta}_{k+1} \\ \eta_0 &= e_0. \end{aligned} \quad (10)$$

Since η_k is unknown, it is necessary to use an estimate, $\hat{\eta}$, which is generated by the recursion:

$$\hat{\eta}_{k+1} = \hat{\eta}_k - K_k \hat{\eta}_k. \quad (11)$$

Let the identifier matrix Σ_k be defined as

$$\Sigma_{k+1} = \alpha \Sigma_k + w_k^T w_k, \quad \Sigma_0 = \alpha I > 0 \quad (12)$$

with an inverse generated by the recursion

$$\Sigma_{k+1}^{-1} = \Sigma_k^{-1} + \left(\frac{1}{\alpha} - 1 \right) \Sigma_k^{-1} - \frac{1}{\alpha^2} \Sigma_k^{-1} w_k (1 + \frac{1}{\alpha} w_k^T \Sigma_k^{-1} w_k)^{-1} w_k^T \Sigma_k^{-1}. \quad (13)$$

Using (7), (8), and (11), the parameter update law is

$$\hat{\theta}_{k+1} = \hat{\theta}_k + \frac{1}{\alpha} \Sigma_k^{-1} \omega_k^T \left(I + \frac{1}{\alpha} w_k \Sigma_k^{-1} w_k^T \right)^{-1} (e_k - \hat{\eta}_k). \quad (14)$$

And to ensure that the parameter estimates remain within the constraint set Θ_k , we use a projection operator (Goodwin and Sin (2013), Guay (2014))

$$\bar{\hat{\theta}}_{k+1} = \text{Proj}\{\hat{\theta}_k + \Sigma_k^{-1} w_k^T (I + w_k \Sigma_k^{-1} w_k^T)^{-1} (e_k - \hat{\eta}_k), \Theta_k\}. \quad (15)$$

The algorithm for the projection operator must be designed to ensure that estimates are bounded within the constraint set and guarantee stability. The design of projection algorithms in discrete-time systems must be done with care—it cannot be designed as in the continuous-time case. A suitable discrete-time projection algorithm is presented in Guay and Burns (2015).

Finally, the proposed control law is given by:

$$u_k = -k_g \hat{\theta}_{1,k} + \hat{u}_k \quad (16)$$

$$\hat{u}_{k+1} = \hat{u}_k - \frac{1}{\tau_I} \hat{\theta}_{1,k} \quad (17)$$

where k_g and τ_I are positive constants to be assigned. One aspect of the proposed adaptive controller (16) is that the quantity $\hat{\theta}_{1,k}$ estimates the term $\theta_{1,k}$ which itself depends on the input. As a result, once estimation of $\theta_{1,k}$ is achieved, the resulting control action defines a recursive map that converges to the implicitly defined state-feedback controller $u_k = \alpha(x_k, \hat{u}_k)$. The proof of convergence provided in Guay and Burns (2015) demonstrates how the effect of the dependence of $\theta_{1,k}$ on u_k can be handled in the design of the PI-ESC.

The final PI-ESC algorithm consists of a time varying parameter estimation routine for determining $\hat{\theta}_{0,k}$ and $\hat{\theta}_{1,k}$ and consists of Equations (7), (8), (11), (13), and (15) with tuning parameters K and α . The control law is given by Equations (16) and (17) and contains terms proportional to the estimated gradient and with integral action necessary to identify optimal equilibrium conditions, and is tuned using the parameters k_g and τ_I . A block diagram of the PI-ESC algorithm summarizing signal flow is shown in Figure 2.

3 COMPARISON OF EXTREMUM SEEKING METHODS

This section presents the convergence performance of three extremum seeking controllers applied to a previously published example problem (Burns *et al.* (2015)). Traditional perturbation-based extremum seeking control (Killingsworth and Krstic (2006)), time-varying extremum seeking control (Guay (2014)) and proportional–integral extremum seeking control (Guay and Burns (2015)) are each applied to the problem of finding input values to a simple Hammerstein system that minimize its output, where the controllers have no knowledge of the plant model (see Fig. 3A). The system equations are

$$\begin{aligned} x_{k+1} &= 0.8x_k + u_k \\ y_k &= (x_k - 3)^2 + 1, \end{aligned}$$

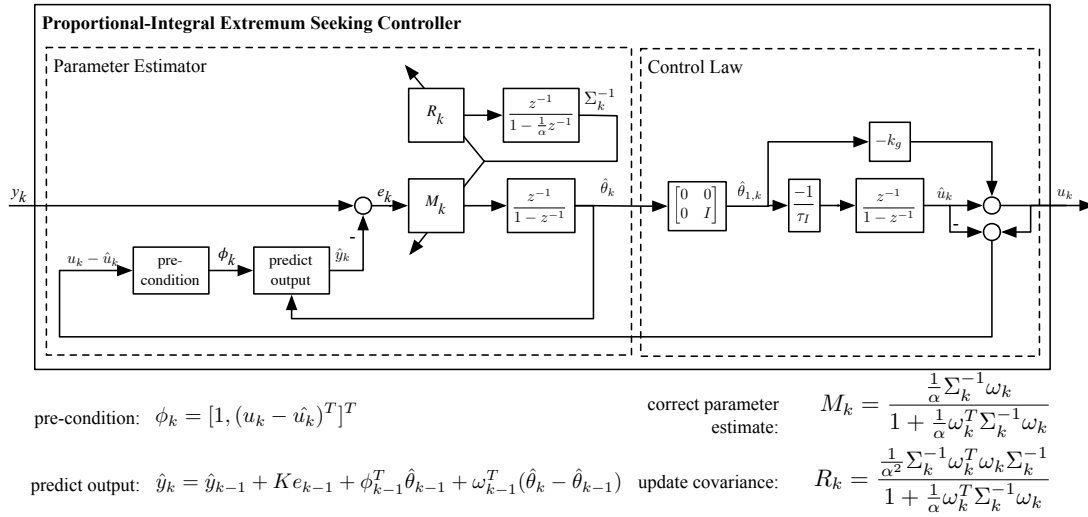


Figure 2: Block diagram of the PI-ESC algorithm.

which has a single optimum point at $u^* = 0.6$, $y^* = 1$.

The pole near the unit circle represents the dominant process dynamics and establishes a fundamental limit on convergence rate. Reasonable effort is made to obtain parameters for all ESC methods that achieve the best possible convergence rates. The perturbation ESC parameters are

$$\begin{aligned} d_k &= 0.2 \sin(0.1k) \\ \omega_{LP} &= 0.03 \\ K &= -0.005 \end{aligned}$$

where d_k is the sinusoidal perturbation, ω_{LP} is the cutoff frequency for a first-order low-pass averaging filter, and K is the (integral-action) adaptation gain. A high-pass washout filter is not used as convergence rate is improved without it.

The parameters used for the TV-ESC are

$$\begin{aligned} d_k &= 0.001 \sin(0.1k) & k_i &= 0.001 \\ \alpha &= 0.1 & \epsilon &= 0.4, \end{aligned}$$

where k_i is the (integral-action) adaptation gain, α is the estimator forgetting factor, and ϵ is the estimator timescale separation parameter.

The parameters used for the PI-ESC are

$$\begin{aligned} d_k &= 0.001 \sin(0.2k) & \tau_I &= 60 \\ \alpha &= 0.5 & k_g &= 0.0003 \\ K &= 0.1, \end{aligned}$$

where τ_I is the integral time constant, k_g is the proportional gain and is computed from the relationship $k_g = 1/(\tau_I^2)$, α is the estimator forgetting factor, and K is the estimation gain.

Simulations are performed starting from an initial input value of $u_0 = 2$ and the ESC methods are turned on after 100 steps. The resulting simulations are shown in Fig. 3B. The perturbation ESC method converges to a neighborhood around the optimum in about 4,000 steps (not shown in the figure), the TV-ESC method converges in about 100 steps, while the PI-ESC method converges in about 15 steps. The resulting controller performance is compared to the

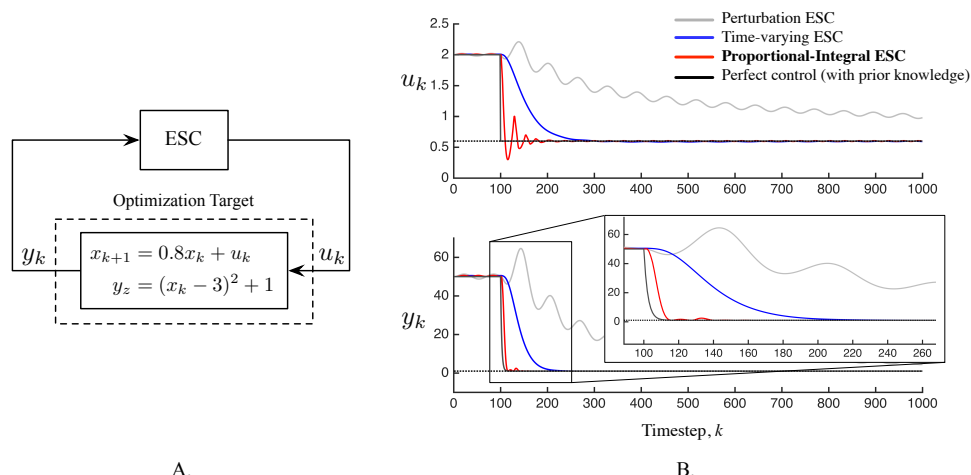


Figure 3: (A) Various extremum seeking control methods are applied to a Hammerstein system. (B) Transient plots compare rate of convergence to the optimizer for various methods. PI-ESC (red) converges in 15 steps or about at the same timescale as the dominant discrete-time system pole (black). Time-varying ESC (blue) converges in about 100 steps whereas perturbation-based ESC (gray) converges in about 4,000 steps.

response obtained from a controller that has *a priori* knowledge of the system optimizer and applied directly in one time step, for which the output settles in about 10 steps. The fast convergence characteristic of PI-ESC is well suited to the optimization of thermal systems with their associated long time constants. In the next section, we apply the PI-ESC algorithm to the problem of selecting setpoints for the discharge temperature of a vapor compression machine and present simulation results.

4 VAPOR COMPRESSION SYSTEM MODEL

A dynamic model of a vapor compression cycle is developed including submodels of its constituent components in order to evaluate the performance of ESC methods in a scenario with realistic physical relationships and time constants. Finite volume models are used to describe the heat exchanger dynamics due to the high spatial and temporal fidelity of that approach. Model assumptions used here include one dimensional fluid flow, no axial heat conduction in the direction of the fluid flow, a homogeneous flow field in the two-phase region, thermodynamic equilibrium in each control volume, dry air composition neglecting humidity, and negligible gravitational forces. A set of simplified closure relations describe the heat transfer and frictional pressure drop using constant phasic heat transfer and a simple power-law relationship between pressure drop and mass flow rate. In addition, a real fluid model is used to define the equations of state for the refrigerant R410a, with the variables of pressure and the mixture-specific enthalpy chosen to represent the fluid state for each control volume. Algebraic models are also used to describe the pressure vs. flow characteristics for the variable speed compressor and expansion valve. Finally, air side dynamics are described by a well-insulated (adiabatic) room wherein a heat source is applied. These models are implemented in Modelica (Modelica Association, 2014); additional details of the system model are available in (Laughman and Qiao, 2015, Laughman *et al.*, 2015).

The compressor rotational speed and expansion valve opening are controlled by decentralized PI controllers (labeled “Feedback Regulator” in Figure 1B), in which the compressor speed loop is closed on room temperature, and the expansion valve loop is closed on discharge temperature. The zone temperature setpoint is held fixed for the subsequent simulations, and the discharge temperature setpoint is determined by the extremum seeking controller. The system equations and the feedback regulator transfer functions are written in continuous time, whereas the extremum seeking controllers are expressed in discrete time. To account for this mixed model type simulation, a synchronous simulation

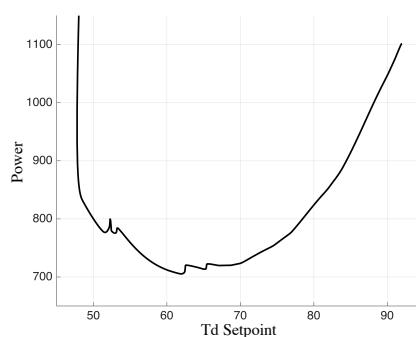


Figure 4: The discharge temperature setpoint is swept in a quasi-steady manner to show the dependency of power consumption on compressor temperature. This steady state map is used as the ground truth to evaluate ESC performance in the next section.

approach is adopted in which the continuous-time portion of the model is integrated forward in time until a clock edge of the discrete-time subsystem is encountered, at which time the extremum seeking controller updates its states and adjusts the control output. The extremum seeking controller is sampled with a period of 60 seconds.

A quasi-steady parameter sweep is performed on the model to illustrate the dependency of power consumption on discharge temperature when other model inputs are fixed. Figure 4 illustrates the resulting steady-state map created by slowly ramping the discharge temperature setpoint from 92°C to 45°C while measuring the resulting power consumption. During this simulation, the outdoor temperature is fixed at 35°C, the indoor air temperature setpoint is 27°C, and the heat load is 2,100 W. The duration of this ramp was set to 70,000 seconds to ensure that the room air temperature would remain within 0.2°C of its setpoint. The resulting dependency is roughly convex and can be understood by considering the system behavior at both extremes. When the discharge temperature is high, the EEV orifice size must be small to reduce the mass flow rate through the compressor and therefore through the evaporator. In order to maintain the required cooling to meet the heat load with this low mass flow rate, the refrigerant must be made colder and therefore the compressor speed is increased, which causes the power consumption to become large at high discharge temperatures. Conversely, at low discharge temperatures two phase refrigerant is ingested in order to reduce the compressor temperature. In this case, much of the potential latent heat gain occurs in the compressor rather than in the conditioned space, which leads to a loss of efficiency.

5 SIMULATION RESULTS

This section describes simulation results wherein various extremum seeking algorithms automatically discover a discharge temperature setpoint that minimizes power consumption for the previously described model of a vapor compression system. In these simulations, the compressor discharge temperature setpoint is modified by the extremum seeking algorithm, while the feedback regulator manipulates the compressor speed, expansion valve and heat exchanger fans in order to achieve these setpoints (refer to Fig. 1B).

Various extremum seeking controllers are applied to a simulation of a vapor compression system tested at the conditions described in the previous section. Initially, the discharge temperature setpoint is set to 92°C, which is about 30°C warmer than the optimal compressor temperature for the conditions tested. The simulation is started with the extremum seeking methods turned off to allow settling of initialization transients. At $t = 15$ min, the extremum seeking controllers are bumplessly switched on.

Figure 5A shows the transient responses of the perturbation based ESC algorithm (in gray), the time-varying ESC algorithm (in blue) and the proportional-integral ESC algorithm (in red). Figure 5B shows the convergence progression for each algorithm plotted against the steady state map (in black). Note that perturbation based ESC follows the map

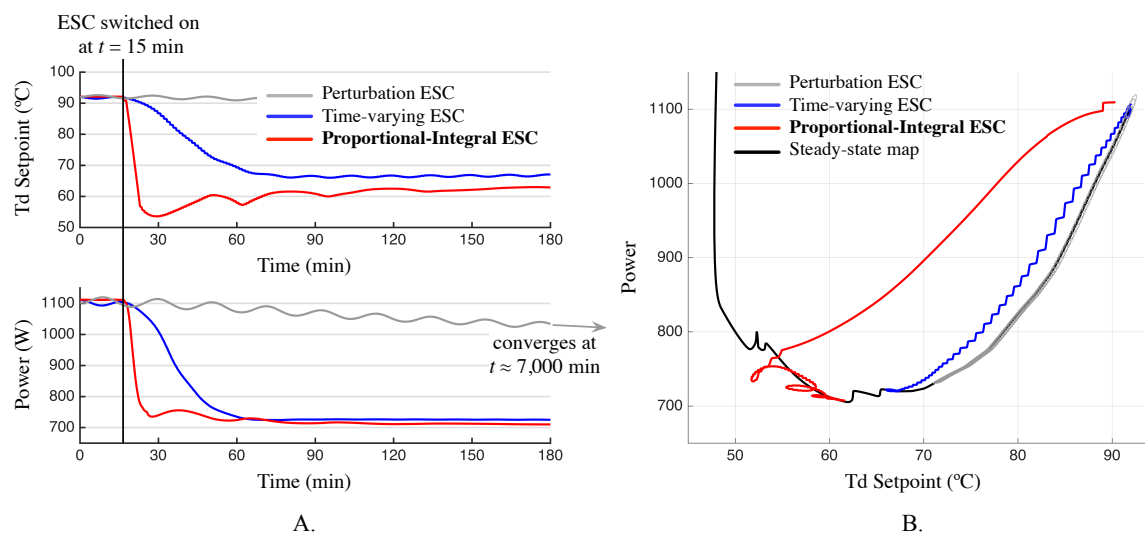


Figure 5: Extremum seeking methods are compared to the problem of finding discharge temperature setpoints that minimize power. Proportional-integral extremum seeking converges substantially faster than other methods.

directly, as this algorithm is a quasi-steady optimization method in which the system dynamics are not excited by design. In contrast, both time-varying ESC and proportional-integral ESC converge away from the steady state map indicating that the vapor compression system dynamics are excited during optimization.

Note that the steady state map is not strictly convex as described in the previous section, and discontinuities in power are apparent for various Td setpoints. When approach slowly from the right (higher Td setpoints), a local minimum is reached at around 68°C for both perturbation based ESC and time-varying ESC. However, the global optimum in this case occurs at 62°C , which is discovered by the proportional-integral extremum seeking controller. Referring to the transient responses of Figure 5A, perturbation based ESC converges to the optimum in around 7,000 min (which is not shown in the figure due to the timescale mismatch), time-varying ESC converges in about 45 minutes after being switched on, and proportional-integral ESC converges in about 15 minutes.

6 CONCLUSION

We have developed a new extremum seeking algorithm that converges at the same timescale as the dominant plant dynamics, which requires an estimation routine designed in conjunction with the proportional-integral control law. With the gradient appropriately estimated, convergence can proceed much faster than alternative approaches. The PI-ESC algorithm is applied to the problem of compressor temperature setpoint selection such that the power consumption is minimized at timescales that can ultimately enable deployment beyond controlled laboratory conditions.

REFERENCES

- Burns, D. and Laughman, C. Extremum Seeking Control for Energy Optimization of Vapor Compression Systems. In *14th International Refrigeration and Air Conditioning Conference at Purdue* (2012).
- Burns, D., Weiss, W., and Guay, M. Realtime Setpoint Optimization with Time-Varying Extremum Seeking for Vapor Compression Systems. In *American Control Conference* (2015).
- Elliott, M.S. and Rasmussen, B.P. On reducing evaporator superheat nonlinearity with control architecture. *International Journal of Refrigeration*, 33(3):607–614 (2010).

- Goodwin, G. and Sin, K. *Adaptive Filtering Prediction and Control*. Dover Books on Electrical Engineering Series. Dover Publications, Incorporated (2013). ISBN 9780486137728.
- Gopal, A.R., Leventis, G., Phadke, A., and du Can, S.d.l.R. Self-financed efficiency incentives: case study of Mexico. *Energy Efficiency*, 7(5):865–877 (2014).
- Guay, M. and Burns, D. A Comparison of Extremum Seeking Algorithms Applied to Vapor Compression System Optimization. In *American Control Conference* (2014).
- Guay, M. and Burns, D. A proportional integral extremum-seeking control approach for discrete-time nonlinear systems. In *IEEE Conference on Decision and Control (CDC)* (2015).
- Guay, M. A time-varying extremum-seeking control approach for discrete-time systems. *Journal of Process Control*, 24(3):98 – 112 (2014).
- Killingsworth, N.J. and Krstic, M. PID tuning using extremum seeking: online, model-free performance optimization. *IEEE Control Systems Magazine*, 26(1):70–79 (2006). ISSN 0272-1708. doi:10.1109/MCS.2006.1580155.
- Krstic, M. Performance Improvement and Limitations in Extremum Seeking Control. *Systems & Control Letters*, 39(5):313–326 (2000).
- Laughman, C. and Qiao, H. Mass conserving models of vapor compression cycles. In *Proceedings of the 11th International Modelica Conference* (2015).
- Laughman, C., Qiao, H., Aute, V., and Radermacher, R. A comparison of transient heat pump cycle models using alternative flow descriptions. *Science and Technology for the Built Environment*, 21(5):666–680 (2015).
- Leblanc, M. Sur l'électrification des chemins de fer au moyen de courants alternatifs de fréquence élevée. *Revue Générale de l'Electricité* (1922).
- Li, P., Li, Y., and Seem, J.E. Efficient Operation of Air-Side Economizer Using Extremum Seeking Control. *Journal of Dynamic Systems, Measurement, and Control*, 132(3) (2010). ISSN 0022-0434. doi:10.1115/1.4001216.
- Modelica Association. Modelica Specification, Version 3.3 (2014).
- Otten, R.J. *Superheat Control for Air Conditioning and Refrigeration Systems: Simulation and Experiments*. Master's thesis, University of Illinois at Urbana-Champaign (2010).
- Sane, H., Haugstetter, C., and Bortoff, S. Building hvac control systems - role of controls and optimization. In *Proceedings of the 2006 American Controls Conference* (2006).
- Tan, Y., Moase, W., Manzie, C., Nesic and, D., and Mareels, I. Extremum seeking from 1922 to 2010. In *29th Chinese Control Conference (CCC)*, pages 14 –26 (2010).
- Tyagi, V., Sane, H., and Darbha, S. An extremum seeking algorithm for determining the set point temperature for condensed water in a cooling tower. In *American Control Conference, 2006*, pages 5 pp.– (2006). doi:10.1109/ACC.2006.1656368.
- Vinther, K., Rasmussen, H., Izadi-Zamanabadi, R., and Stoustrup, J. Single temperature sensor superheat control using a novel maximum slope-seeking method. *International Journal of Refrigeration*, 36(3):1118–1129 (2013).
- Weiss, W., Burns, D., and Guay, M. Realtime Optimization of MPC Setpoints using Time-Varying Extremum Seeking Control for Vapor Compression Machines. In *15th International Refrigeration and Air Conditioning Conference at Purdue* (2014).